

Article

Characterization of Rare Events in Molecular Dynamics

Carsten Hartmann^{1,*}, Ralf Banisch¹, Marco Sarich¹, Tomasz Badowski¹ and C. Schütte^{1,2}

¹ Institut für Mathematik, Freie Universität Berlin, Arnimallee 6, 14195 Berlin, Germany

² Konrad-Zuse Zentrum, Takustraße 7, 14195 Berlin, Germany

* Author to whom correspondence should be addressed; E-Mail, Tel. and Fax number of the corresponding author.

Version July 23, 2013 submitted to *Entropy*. Typeset by *LaTeX* using class file *mdpi.cls*

Abstract: A good deal of molecular dynamics simulations aims at predicting and quantifying rare events, such as the folding of a protein or a phase transition. Simulating rare events is often prohibitive, especially if the equations of motion are high-dimensional, as is the case in molecular dynamics. Various algorithms have been proposed for efficiently computing mean first passage times, transition rates or reaction pathways. This article surveys and discusses recent developments in the field of rare event simulation and outlines a new approach that combines ideas from optimal control and statistical mechanics. The optimal control approach described in detail resembles the use of Jarzynski's equality for free energy calculations, but with an optimized protocol that speeds up the sampling, while (theoretically) giving variance-free estimators of the rare events statistics. We illustrate the new approach with two numerical examples and discuss its relation to existing methods.

Keywords: rare events, molecular dynamics, optimal pathways, stochastic control, dynamic programming, change of measure, cumulant generating function

1. Introduction

Rare but important transition events between long lived states are a key feature of many systems arising in physics, chemistry, biology, etc. Molecular dynamics (MD) simulations allow for analysis and understanding of the dynamical behaviour of molecular systems. However, realistic simulations for interesting (large) molecular systems in solution on timescales beyond microseconds are still infeasible even on the most powerful general purpose computers. This significantly limits the MD-based analysis of many biological equilibrium processes, because they often are associated with rare events. These rare

21 events require prohibitively long simulations because the average waiting time between the events is
22 orders of magnitude longer than the timescale of the transition characterizing the event itself. Therefore,
23 the straightforward approach to such a problem via direct numerical simulation of the system until a
24 reasonable number of events has been observed is impractically excessive for most interesting systems.
25 As a consequence rare event simulation and estimation are among the most challenging topics in
26 molecular dynamics.

27 In this article we consider typical rare events in molecular dynamics for which conformation changes
28 or protein folding may serve as examples. They can be described in the following abstract way: The
29 molecular system under consideration has the ability to go from a reactant state given by a set A in its
30 state space (e.g. an initial conformation) to a product state described by another set B (e.g. the target
31 conformation). Dynamical transitions from A to B are rare. The general situation we will address is as
32 follows:

- 33 • The system is (meta)stable, with the sets A and B being two of its metastable sets in the sense that
34 if the system is put there it will remain there for a long time; transitions between A and B are rare
35 events.
- 36 • The sets A and B are separated by an unknown and, in general, rough or diffusive energy landscape
37 (that will be denoted by V).

In addition, we will assume that the system under consideration is in equilibrium with respect to the stationary probability density

$$\mu(x) = \frac{1}{Z} \exp(-\beta V(x)).$$

38 We are interested in characterizing the transitions leading from A into B , that is, we are interested in the
39 statistical properties of the ensemble of *reactive trajectories* that go *directly* from A to B (i.e. start in A
40 without returning to A before going to B). In other words we are interested in all trajectories comprising
41 the actual transition. We would like to

- 42 • know which parts of state space such reactive trajectories visit most likely, i.e., where in state
43 space do we find transition pathways or transition channels through which most of the probability
44 current generated by reactive trajectories flows, and
- 45 • characterize the rare event statistically, i.e. compute the transition rate, the free energy barrier, the
46 mean first passage time or even more elaborated statistical quantities.

47 The molecular dynamics literature on rare event simulations is rich. Since the 1930s transition state
48 theory (TST) [1,2] and extensions thereof based on the reactive flux formalism have provided the main
49 theoretical framework for the description of transition events. TST can, however, at best deliver rates and
50 does not allow to characterize transition channels. It is based on partitioning the state space into two sets
51 with a dividing surface in between, leaving set A on one side and the target set B on the other, and the
52 theory only tells how this surface is crossed during the reaction. Often, it is difficult to choose a suitable
53 dividing surface and a bad choice will lead to a very poor estimate of the rate. The TST estimate is then
54 extremely difficult to correct, especially if the rare event is of the diffusive type where many different
55 reaction channels co-exist. Therefore, many techniques have been proposed that try to go beyond TST.

56 These different strategies approach the problem by sampling the ensemble of reactive trajectories or
57 by directly searching for the transition channels of the system. Most notable among these techniques are
58 (1) Transition Path Sampling (TPS) [3], (2) the so-called String Methods [4], or optimal path approaches
59 [5–7] and variants thereof, and (3) techniques that follow the progress of the transition through interfaces
60 like Forward-Flux Simulation (FFS) [8], Transition Interface Sampling (TIS) [9], or the Milestoning
61 techniques [10,11], and (4) methods that drive the molecular system by external forces with the aim
62 of making the required transition more frequent while still allowing to compute the exact rare event
63 statistics for the unforced system, e.g. based on Jarzynski’s and Crook’s identity [12,13]. All of these
64 methods consider the problem in continuous state space, i.e. through reactive trajectories or transition
65 channels in the original state space of the molecular system. They all face substantial problems, e.g. if
66 the ensemble of reactive trajectories and/or transition channels of the system under consideration are too
67 complicated (multi-modal, irregular, essentially high dimensional), or they suffer from too large variance
68 of the underlying statistical estimators.

69 Our aim is (A) to review some of these methods based on a joint theoretical basis, and (B) to outline
70 a new approach to the estimation of rare event statistics based on a combination of ideas from optimal
71 control and statistical mechanics. In principle this approach allows for a *variance-free* estimation of rare
72 event statistics in combination with *much reduced simulation time*. The rest of the article is organized as
73 follows: We start with a precise characterization of reactive trajectories, transition channels and related
74 quantities in the framework of Transition Path Theory (TPT) in Section 2. Then, in Sections 3–4, we
75 discuss the methods from classes (1)–(3) and characterize their potential problems in more detail. In
76 Section 5 we consider methods of type (4) as an introduction to the presentation of the new optimal
77 control approach that is outlined in detail in Sections 6–7, including some numerical experiments.

78 Alternative, inherently discrete methods like Markov State Modelling that discretize the state space
79 appropriately and try to compute transition channels and rates a posteriori based on the resulting discrete
80 model of the dynamics will not be discussed herein and are considered in the article [14] in a way related
81 to the presentation at hand.

82 2. Reactive Trajectories, Transition Rates, and Transition Channels

83 Since our results are rather general, it is useful to set the stage somewhat abstractly. We shall consider
84 a system whose state space is \mathbb{R}^n and denote by X_t the current state of the system at time t . For example,
85 X_t may be the set of instantaneous positions and momenta of the atoms of a molecular system. We
86 assume that the system is ergodic with respect to a probability (equilibrium) distribution μ , and that we
87 can generate an infinitely long equilibrium trajectory $\{X_t\}_{t \geq 0}$. The trajectory will go infinitely many
88 times from A to B , and each time the reaction happens. This reaction involves reactive trajectories that
89 can be defined as follows: Given the trajectory $\{X(t)\}_{t \geq 0}$, we say that its reactive pieces are the segments
90 during which X_t is neither in A or B , came out of A last and will go to B next. To formalize things, let

$$\begin{aligned} t_{AB}^+(t) &= \text{smallest } s \geq t \text{ such that } X(s) \in A \cup B \\ t_{AB}^-(t) &= \text{largest } s \leq t \text{ such that } X(s) \in A \cup B \end{aligned}$$

Then the trajectory $\{X(t)\}_{t \geq 0}$ is reactive for all $t \in R$ where $R \subset [0, \infty)$ is defined by the requirements

$$X_t \notin A \cup B, \quad X_{t_{AB}^+(t)} \in B \quad \text{and} \quad X_{t_{AB}^-(t)} \in A,$$

and the ensemble of reactive trajectories is given by the set

$$\mathcal{R} = \{X_t: t \in R\},$$

91 where each specific continuous piece of trajectory going directly from A to B in the ensemble belongs
92 to a specific interval $[t_1, t_2] \subset R$.

93 Given the ensemble of reactive trajectories we want to characterize it statistically by answering the
94 following questions:

95 (Q1) What is the probability of observing a trajectory at $x \notin (A \cup B)$ at time t , conditional on $t \in R$?

96 (Q2) What is the probability current of reactive trajectories? This probability current is the vector field
97 $j_{AB}(x)$ with the property that given any separating surface S between A and B (i.e. the boundary
98 of a region that contains A but not B), the surface integral of j_{AB} over S gives the probability flux
99 of reactive trajectories between A and B across S .

100 (Q3) What is the transition rate of the reaction, i.e. what is the mean frequency k_{AB} of transitions from
101 A to B ?

102 (Q4) Where are the main transition channels used by most of the reactive trajectories?

Question (Q1) can be answered easily, at least theoretically: The probability density to observe any trajectory (reactive or not) at point x is $\mu(x)$. Let $q(x)$ be the so-called committor function, that is the probability that the trajectory starting from x reaches first B rather than A . If the dynamics is reversible, then the probability that a trajectory we observe at state x is reactive is $q(x)(1 - q(x))$, where the first factor appears since the trajectory must go to B rather than A next, and the second factor appears since it needs to come from A rather than B last. Now the Markov property of the dynamics implies that the probability density to observe a *reactive* trajectory at point x is

$$\mu_{AB}(x) \propto q(x)(1 - q(x)) \mu(x),$$

103 which is the probability of observing any trajectory in x times the probability that it will be reactive (the
104 proportionality symbol \propto is used to indicate identity up to normalization).

105 2.1. Transition Path Theory (TPT)

In order to give answers to the other questions, we will exploit the framework of *transition path theory* (TPT) which has been developed in [15–18] in the context of diffusions and has been generalized to discrete state spaces in [19,20]. In order to review the key results of TPT let us consider diffusive molecular dynamics in an energy landscape $V: \mathbb{R}^n \rightarrow \mathbb{R}$:

$$dX_t = -\nabla V(X_t)dt + \sqrt{2\epsilon} dB_t, \quad X_0 = x. \quad (1)$$

106 Here B_t denotes standard n -dimensional Brownian motion, and $\epsilon > 0$ is the temperature of the system.
 107 Under mild conditions on the energy landscape function V we have ergodicity with respect to the
 108 stationary distribution $\mu(x) = Z^{-1} \exp(-\beta V(x))$ with $\beta = 1/\epsilon$. The dynamics is reversible with respect
 109 to this distribution, i.e. the detailed balance condition holds. We assume throughout that the temperature
 110 is small relative to the largest energy barriers, i.e., $\epsilon \ll \Delta V_{\max}$. As a consequence, the relaxation of the
 111 dynamics towards equilibrium is dominated by the rare transitions over the largest energy barriers.

For this kind of dynamics, questions (Q2) and (Q3) have surprisingly simple answers: The reactive probability current is given by

$$j_{AB}(x) = \epsilon \mu(x) \nabla q(x),$$

where ∇q denotes the gradient of the committor function q . Based on this, the transition rate can be computed by the total reactive current across an arbitrary separating surface S :

$$k_{AB} = \int_S n_S(x) j_{AB}(x) d\sigma_S(x)$$

where n_S denote the unit normal vector on S pointing towards B and σ_S the associated surface element. The rate can also be expressed by

$$k_{AB} = \epsilon \int_{(A \cup B)^c} (\nabla q(x))^2 \mu(x) dx,$$

where $(A \cup B)^c$ denotes the entire state space excluding A and B . Given the reactive current, we can even answer question (Q4): The transition channels of the reaction $A \rightarrow B$ are the regions of $(A \cup B)^c$ in which the streamlines of the reactive current, i.e. the solutions of

$$\frac{d}{dt} x_{AB}(t) = j_{AB}(x_{AB}(t)), \quad x_{AB}(0) \in A$$

112 are exceptionally dense.

113 Figure 1 illustrates these quantities for the case of a 2d three well potential with two main wells (the
 114 bottoms of which we take as A and B in the following) and a less significant third well. The three
 115 main saddle points separating the wells are such that the two saddle points between the main wells
 116 and the third well are lower in energy than the saddle point between the main wells, such that in the
 117 zero temperature limit we expect that almost all reactive trajectories take the route through the third
 118 well across the two lower saddle points. We observe that the committor functions for low and higher
 119 temperatures exhibit smooth isocommittor lines separating the sets A and B , as expected. The transition
 120 channels computed from the associated reactive current also show what one should expect: For lower
 121 temperature the channel through the third well and across the two lower saddle points is dominant, while
 122 for higher temperature, the direct transition from A to B across the higher saddle point is preferred.

123 These considerations can be generalized to a wide range of different kinds of dynamics in continuous
 124 state spaces including e.g. full Langevin dynamics, see [15–18].

This example illustrates that TPT in principle allows to quantify all aspects of the transition behavior underlying a rare event. We can compute transition rates exactly and even characterize the transition mechanisms if we can compute the committor function. Deeper insight using the Feynman-Kac formula

yields that the committor function can be computed as the solution of a linear boundary value problem, which for diffusive molecular dynamics reads

$$Lq_{AB} = 0 \quad \text{in } (A \cup B)^c, \quad q_{AB} = 0 \text{ in } A, \quad q_{AB} = 1 \text{ in } B,$$

where the generator L has the following form

$$L = \epsilon\Delta - \nabla V(x) \cdot \nabla, \quad (2)$$

125 where $\Delta = \sum_i \partial^2 / \partial x_i^2$ denotes the Laplace operator. This equation allows the computation of q_{AB}
 126 in relatively low-dimensional spaces, where the discretization of L is possible based on finite element
 127 methods or comparable techniques. In realistic biomolecular state spaces this is infeasible because of
 128 the curse of dimensionality. Therefore, TPT gives a complete theoretical background for rare event
 129 simulation but its application in high dimensional situations is still problematic. As a remedy, a discrete
 130 version of TPT has been developed [19,20], which can be used in combination with Markov State
 131 Modelling, see [21].

132 2.2. Transition Path Sampling (TPS)

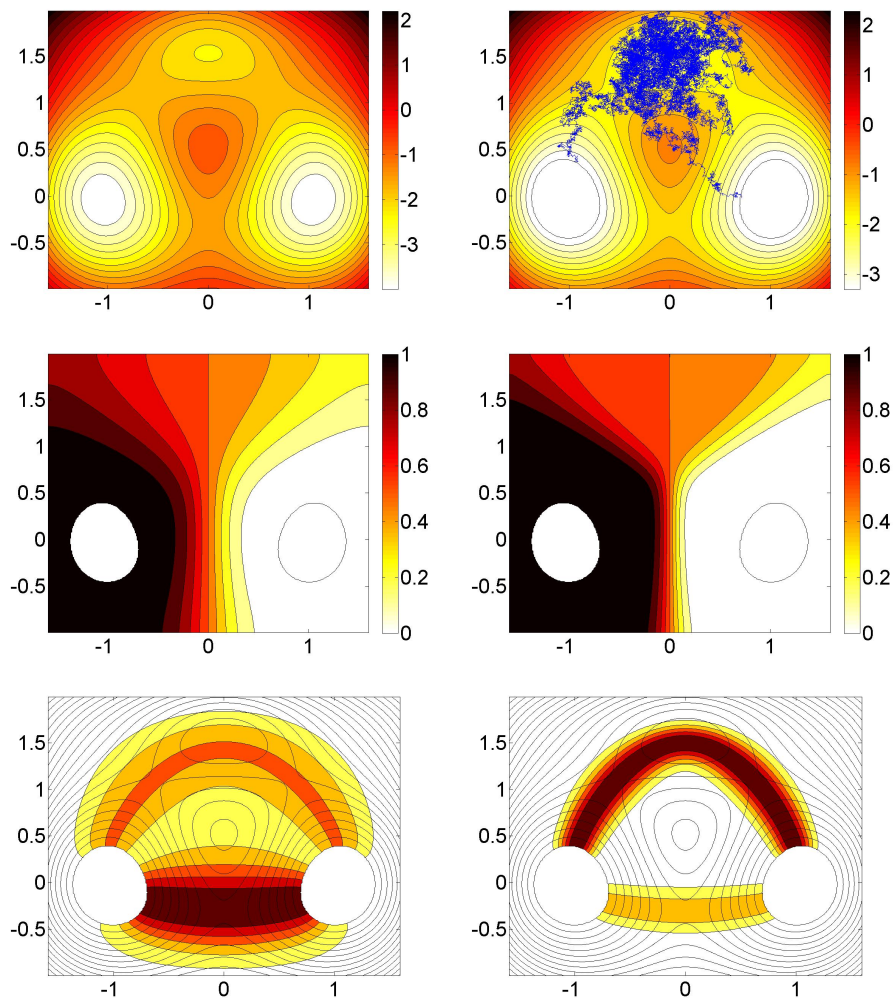
TPS has been developed in order to sample from the probability distribution of reactive trajectories in so-called "path space", which means nothing else than the space of all discrete or continuous paths starting in A and ending up in B equipped with the probability distribution generated by the dynamics through the ensemble of associated reactive trajectories. Let P_T denote the path measure on the space of discrete or continuous trajectories $\{X_t\}_{0 \leq t \leq T}$ of length T . The *path measure of reactive trajectories* then is

$$P_T^{AB}(\{X_t\}_{0 \leq t \leq T}) = \frac{1}{Z_{AB}} \mathbf{1}_A(X_0) P_T(\{X_t\}_{0 \leq t \leq T}) \mathbf{1}_B(X_T),$$

133 where $\mathbf{1}_A$ denotes the indicator function of set A (that is, $\mathbf{1}_A(x) = 0$ if $x \notin A$ and $= 1$ otherwise).

134 TPS is a Metropolis Monte-Carlo (MC) method for sampling $P_T^{AB}(\{X_t\}_{0 \leq t \leq T})$ that exploits explicit
 135 information like (3) regarding the path measure P_T [22,23]. It delivers an ensemble of reactive
 136 trajectories of length T that (under the assumption of convergence of the MC scheme) is representative
 137 for P_T^{AB} and thus allows to compute respective expectation values like the probability to observe a
 138 reactive trajectory or the reactive current. However, its potential drawbacks are obvious: (1) A typical
 139 reactive trajectory is very long and rather uninformative (cf. Fig. 1), i.e. the computational effort of
 140 generating an entire ensemble of long reactive trajectories can be prohibitive, (2) convergence of the
 141 MC scheme in the extremely high dimensional path spaces can be very poor, and (3) the limitation to a
 142 pre-defined trajectory length T can lead to biased statistics of the TPS ensemble. Advanced TPS schemes
 143 try to remedy these drawbacks by combining the original TPS idea with interface methods [9].

Figure 1. Top left panel: Three-well energy landscape V as described in the text. Top right panel: Typical reactive trajectory in the three-well landscape. Middle left panel: Committor functions q_{AB} for diffusion molecular dynamics with relatively high temperature $\epsilon = 0.6$ for the sets A (main well, right hand side) and B (main well, left hand side). Middle right panel: Committor q_{AB} for the low temperature case $\epsilon = 0.15$. Bottom left panel: Transition channels for $\epsilon = 0.6$. Bottom right panel: Transition channels for $\epsilon = 0.15$. For details of the computations underlying the pictures see [20].



144 3. Finding Transition Channels

145 Whenever a transition channel exists, one can try to approximate the principal curve in the center of
 146 the transition channel instead of sampling the ensemble of reactive trajectories. If this principal curve
 147 is a rather smooth object then such a method would not suffer from the extensive length of reactive
 148 trajectories. Several such methods have been introduced; they differ with respect to the definition of the
 149 principal curve.

150 3.1. Action-based Methods

Rather than sampling the probability distribution of reactive pathways, one can try to obtain a representative or *dominant* pathway, e.g. by computing the pathway that has maximum probability under P_T . For the case of diffusive molecular dynamics the path measure P_T has a probability density with respect to a (fictitious) uniform measure on the space of all continuous paths in \mathbb{R}^n , which reads

$$\ell(\varphi) = \exp\left(-\frac{1}{2\epsilon}I_\epsilon(\varphi)\right),$$

where I_ϵ is the Onsager-Machlup action

$$I_\epsilon(\varphi) = \int_0^T \left\{ \frac{1}{2}|\dot{\varphi}(s)|^2 + \frac{1}{2}|\nabla V(\varphi(s))|^2 - \epsilon\Delta V(\varphi(s)) \right\} dt. \quad (3)$$

151 The form of the path density ℓ has led to the idea that by minimizing the Onsager-Machlup action
 152 over all continuous paths $\varphi: [0, T] \rightarrow \mathbb{R}^n$ going from A to B one can find the dominant reactive path
 153 $\varphi^* = \operatorname{argmin}_\varphi I_\epsilon(\varphi)$, often also called optimal path or most probable path. The hope is that this path on
 154 one hand contains information on the transition mechanism and on the other hand is much smoother and
 155 easier to interpret than a typical reactive trajectory.

156 In [7] a direct approach to this question using gradient descent methods has been given for diffusive
 157 molecular dynamics, raising issues regarding the correct interpretation of the minimizers of I_ϵ (that need
 158 not exist) as *most probable paths*. In [5] the *dominant reaction pathway method* has been outlined which
 159 uses a simplified version of the Onsager-Machlup functional that leads to a computationally simpler
 160 optimization problem and is applicable to large-scale problems, e.g., protein folding [6]. But even if the
 161 globally dominant pathways can be computed and the optimization does not get stuck in local minima,
 162 the resulting pathways in general do *not* allow to gain statistical information on the transition (like rates,
 163 currents, mean first passage times).

Another action-based method that has been introduced in [24] is the *MaxFlux* method which seeks the path that carries the highest reactive flux among all reactive trajectories of a certain length. The idea is to compute the path of least resistance by minimizing the functional

$$L(\varphi) = \int_0^T \exp(\epsilon^{-1}V(\varphi(s))) ds.$$

164 Several algorithmic approaches for the minimization of the resistance functional L have been proposed,
 165 e.g. a path-based method [25], discretization of the corresponding Euler-Lagrange equation based
 166 on a mean-field approximation of it [26] or a Hamilton-Jacobi-based approach using the method of

167 characteristics [27]. Minimizing L for different values of T then yields a collection of paths, each of
 168 which carries a certain percentage of the total reactive flux. The method is useful if the temperature is
 169 small, so that the reactive flux concentrates around a sufficiently small number of reactive pathways.

170 3.2. String Method and Variants

There are several other methods that entirely avoid the computation of reactive trajectories but try to reconstruct the less complex transition channels or pathways instead, analysing the energy landscape of the system. One group of such techniques like the Zero Temperature String method [28] or the Nudged Elastic Band method [29] concentrate on the computation of the *minimal energy path* (MEP), i.e. the path of lowest potential energy between (a point in) A and (a point in) B . Under diffusive molecular dynamics and for vanishing temperature the MEP is the path that transitions take with probability one [30]. It turns out that the MEP in this case is the minimizer of the Onsager-Machlup action (3) in the limit $\epsilon \rightarrow 0$. For non-zero temperature and a rugged energy landscape the MEP will in general be not very informative and must be replaced by a finite-temperature transition channel. This is done by the finite-temperature string (FTS) method [31] based on the following considerations: Firstly, the isocommittor surfaces Γ_α , $\alpha \in [0, 1]$, of the committor q are taken as natural interfaces that separate A from B . Secondly, each Γ_α is weighted with the stationary distribution μ to find reactive trajectories crossing it at a certain point $x \in \Gamma_\alpha$,

$$\rho_\alpha(x) = \frac{1}{Z_\alpha} q(x)(1 - q(x)) \mu(x), \quad Z_\alpha = \int_{\Gamma_\alpha} q(x)(1 - q(x)) \mu(x) d\sigma_\alpha(x).$$

171 The idea of the FTS method is that the ensemble of reactive trajectories can be characterized by this
 172 distribution on the isocommittor surfaces. Third, one assumes that for each α the probability density ρ_α
 173 is peaked in just one point $\varphi(\alpha)$ and that the curve $\varphi = \varphi(\alpha)$, $\alpha \in [0, 1]$ defined by the sequence of these
 174 points forms the center of the (single) transition channel. More precisely, one defines $\varphi(\alpha) = \langle x \rangle_{\Gamma_\alpha}$
 175 where the average is taken according to ρ_α along the respective isocommittor surface Γ_α . Fourth, it
 176 is assumed that the covariance $C_\alpha = \langle (x - \varphi(\alpha)) \otimes (x - \varphi(\alpha)) \rangle_{\Gamma_\alpha}$ —which defines the width of the
 177 transition channel—is small, which implies that the isocommittor surfaces can be locally approximated
 178 by hyperplanes P_α . The computation of the FTS string φ then is done by approximating it via $\varphi(\alpha) =$
 179 $\langle x \rangle_{P_\alpha}$, where the average is computed by running constrained dynamics on P_α while iteratively refining
 180 the hyperplanes P_α ; see [32] for details. Later extensions [33] remove the restrictions resulting from the
 181 hyperplanes by using Voronoi tessellations instead.

The FTS method allows to compute single transition channels in rugged energy landscapes as long as these are not too extended and rugged. Compared to methods that sample the ensemble of reactive trajectories, it has the significant advantage that the string—that is, the principal curve inside the transition channel—is rather smooth and short, as compared to the typical reactive trajectories. The FTS further allows to compute the free energy profile $F = F(\alpha)$ along the string,

$$F(\alpha) = -\beta^{-1} \log \int_{P_\alpha} \mu(x) d\sigma_\alpha(x),$$

182 that characterizes the transition rates associated with the transition channel (at least in the limits of the
 183 approximations invoked by the FTS).

184 4. Computing Transition Rates

185 The computation of transition rates can be performed without computing the dominant transition
 186 channels or similar objects. There is a list of rather general techniques, with Foward Flux Sampling
 187 (FFS) [8], Transition Interface Sampling (TIS) [9] and Milestoning [10] as examples, that approximate
 188 transition rates by exploring how the transition progresses from one to the next interface that separate A
 189 from B .

190 4.1. Forward Flux Sampling (FFS)

The first step of FFS is the choice of a finite sequence of interfaces I_k , $k = 1, \dots, N$, in state space between A and $B = I_N$. The transition rate k_{AB} comes as the product of two factors: (1) the probability current J_A of *all* trajectories leaving A and hitting I_1 , and (2) the probability

$$\mathbb{P}(B|I_1) = \prod_{j=1}^{N-1} \mathbb{P}(I_{k+1}|I_k)$$

191 that a trajectory that leaves I_1 makes it to B before it returns to A ; here $\mathbb{P}(I_{k+1}|I_k)$ denotes the probability
 192 that a trajectory starting in I_k makes it to I_{k+1} before it returns to A . FFS first performs a brute-force
 193 simulation starting in A which yields an ensemble of points at the first interface I_1 yielding an estimate
 194 for the flux J_A (the number of trajectories hitting I_1 per unit of time). Second a point from this ensemble
 195 on I_1 is selected at random and used to start a trajectory which is followed until it either hits the next
 196 interface I_2 or returns to A ; this gives $\mathbb{P}(I_2|I_1)$. This procedure then is iterated from interface to interface.
 197 Finally the rate $k_{AB} = J_A \cdot \mathbb{P}(B|I_1)$ is computed. Variants of this algorithm are described in [34] and
 198 [35], for example.

199 FFS has been demonstrated to be quite general in approximating the flux of reactive trajectories
 200 through a given set of interfaces; it can be applied to equilibrium as well as non-equilibrium systems
 201 and its implementation is easy. The interfaces used in FFS are, in principle, arbitrary. However, the
 202 efficiency of the sampling of the reactive hitting probabilities $\mathbb{P}(I_{k+1}|I_k)$ crucially depends on the choice
 203 of the interfaces. In practice the efficiency of FFS will drop dramatically if one does not use appropriate
 204 surfaces, and totally misleading rates may result from this. Ideally, one would like to choose these
 205 surfaces so as to optimize the computational gain offered by FFS, but how to do so is not clear. The
 206 same is true for TIS that couples TPS with progressing from interface to interface.

207 4.2. Milestoning Milestoning [10] is similar to FFS in so far as it also uses a set of interfaces I_k ,

208 $k = 1, \dots, N$ that separate A and $B = I_N$. In contrast to FFS and TIS, the fundamental quantities in
 209 Milestoning are the hitting time distributions $K_i^\pm(\tau)$, $i = 1, \dots, N - 1$, where $K_i^\pm(\tau)$ is the probability
 210 that a trajectory starting at $t = 0$ at interface I_i hits $I_{i\pm 1}$ before time τ . Trajectories that make it to
 211 milestone I_i must come from milestones $I_{i\pm 1}$, and vice versa. In the original algorithm these distributions
 212 are approximated as follows [10]: For each milestone I_i one first samples the distribution μ constrained
 213 to I_i . Based on the resulting sample, we start a trajectory from each point which is terminated when it

214 reaches one of its two neighboring milestones $I_{i\pm 1}$. The hitting times are recorded and collected into two
 215 distributions $K_i^\pm(\tau)$.

216 These local kinetics are then compiled into the global kinetics of the process: For each i , one defines
 217 $P_i(t)$ as the probability that the process is found between I_{i-1} and I_{i+1} at time t and that the last milestone
 218 hit was I_i . Milestoning is based on a (non-Markovian) construction of $P_i(t)$ from the $K_i^\pm(\tau)$. Its
 219 efficiency comes from two sources: (1) It does not require the computation of long reactive trajectories
 220 but only short ones between milestones (which therefore should be 'close enough'). (2) It is easily
 221 parallelizable. Its disadvantage is the dependence on the milestones that have to be chosen in advance:
 222 It can be shown that Milestoning with perfect sampling allows to compute exact transition rates or mean
 223 first passage times if the interfaces are given by the isocommittor surfaces (which in general are not
 224 known in advance) [36]; if the interfaces are chosen inappropriately the results can be rather misleading.

225 5. Nonequilibrium Forcing and Jarzynski's Identity

226 The computation of reliable rare event statistics suffers from the enormous lengths of reactive
 227 trajectories. One obvious way to overcome this obstacle is to force the system to exhibit the transition
 228 of interest on shorter timescales. So can we *drive* the molecular system to make the required transition
 229 more frequently but still compute the exact rare event statistics for the unforced system?

230 As was shown by Jarzynski and others, nonequilibrium forcing can in fact be used to obtain
 231 equilibrium rare event statistics. The advantage seems to be that the external force can speed up the
 232 sampling of the rare events by biasing the equilibrium distribution towards a distribution under which
 233 the rare event is no longer rare. We will shortly review Jarzynski's identity before discussing the matter
 234 in more detail.

5.1. *Jarzynski's Identity* Jarzynski's and Crook's formulae [12,13] relate the equilibrium Helmholtz free energy to the nonequilibrium work exerted under external forcing: Given a system with energy landscape $V(x)$, the total Helmholtz free energy can be defined as

$$F = -\beta^{-1} \log Z \quad \text{with} \quad Z = \int \exp(-\beta V(x)) dx .$$

Jarzynski's equality [12] then relates the free energy difference $\Delta F = -\beta^{-1} \log(Z_1/Z_0)$ between two equilibrium states of a system given by an unperturbed energy V_0 and its perturbation V_1 with the work W applied to the system under the perturbation: Suppose we set $V_\xi = (1 - \xi)V_0 + \xi V_1$ with $\xi \in [0, 1]$, and assume we set a protocol that describes how the system evolves from $\xi = 0$ to $\xi = 1$. If, initially, the system is distributed according to $\exp(-\beta V_0)$ then, by the second law of thermodynamics, it follows that $\mathbf{E}(W) \geq \Delta F$ where W is the total work applied to the system and \mathbf{E} denotes the average over all possible realizations of the transition from $\xi = 0$ to $\xi = 1$; equality is attained if the transition is infinitely slow (i.e., adiabatically). Jarzynski's identity now asserts that

$$\Delta F = -\beta^{-1} \log \mathbf{E} \left[\exp(-\beta W) \right] .$$

235 Many generalizations exist: In [13], a generalized version of this fluctuation theorem, the so-called
 236 Crook's formula, for stochastic, microscopically reversible dynamics is derived. In [37,38] it is shown

237 how one can compute conditional free energy profiles along a reaction coordinate for the *unperturbed*
 238 system, rather than total free energy differences between perturbed and unperturbed system.

239 **Algorithmic application prohibitive.** Despite the fact that Jarzynski's and Crook's formulae are
 240 used in molecular dynamics applications [39], their algorithmic usability is limited by the fact that
 241 the likelihood ratio between equilibrium and nonequilibrium trajectories is highly degenerate, and the
 242 overwhelming majority of nonequilibrium forcings generate trajectories that have almost zero weight
 243 with respect to the equilibrium distribution that is relevant for the rare event. This leads to the fact that
 244 most rare event sampling algorithms based on Jarzynski's identity have *prohibitively large variance*.
 245 Recent developments have reduced this problem by sampling just the reversible work processes based
 246 on Crook's formula but could not fully remove the problem of large variance. Because of this, we will
 247 approach the problem of variance reduction subsequently.

248 5.2. Cumulant Generating Functions

In order to demonstrate how to improve approaches based on the idea of driving molecular systems to make rare events frequent, we first have to introduce some concepts and notation from statistical mechanics: Let W be a random variable that depends on the sample paths of $(X_t)_{t \geq 0}$, i.e. on molecular dynamics trajectories of the system under investigation. Further let P be the underlying probability measure on the space of continuous trajectories as introduced in Section 2.2 (but without the restriction to a given length T). We define the *cumulant generating function* (CGF) of W by

$$\gamma(\sigma) = -\sigma^{-1} \log \mathbf{E}[\exp(-\sigma W)], \quad (4)$$

where σ is a non-zero scalar parameter and $\mathbf{E}[f] = \int f dP$ denotes the expectation value with respect to P . Note that the CGF is basically the free energy at inverse temperature β as in Jarzynski's formula, but here is considered as a function of the independent parameter σ .¹ Taylor expanding the CGF about $\sigma = 0$, we observe that $\gamma(\sigma) \approx \mathbf{E}[W] - \frac{\sigma}{2} \mathbf{E}[(W - \mathbf{E}[W])^2]$, hence, for sufficiently small σ , the variance is decoupled from the mean. Moreover it follows by Jensen's inequality that

$$\gamma(\sigma) \leq \mathbf{E}[W],$$

249 where equality is achieved if and only if W is almost surely constant, in accordance with the second law
 250 of thermodynamics.²

Optimal reweighting The CGF admits a variational characterization in terms of relative entropies. To this end let Q be another probability measure so that P is absolutely continuous with respect to Q , i.e. the likelihood ratio dP/dQ exists and is Q -integrable. Then, using Jensen's inequality again,

$$\begin{aligned} -\sigma^{-1} \log \int e^{-\sigma W} dP &= -\sigma^{-1} \log \int e^{-\sigma W + \log(\frac{dP}{dQ})} dQ \\ &\leq \int \left\{ W + \sigma^{-1} \log \left(\frac{dQ}{dP} \right) \right\} dQ, \end{aligned}$$

¹Definition (4) differs from the standard CGF only by the prefactor σ^{-1} in front.

²This is the case, e.g., when W is the work associated with an adiabatic transition between thermodynamic equilibrium states.

which, noting that the logarithmic term is the relative entropy (or Kullback-Leibler divergence) between Q and P , can be recast as

$$\gamma(\sigma) \leq \int W dQ + H(Q\|P). \quad (5)$$

where

$$H(Q\|P) = \sigma^{-1} \int \log \left(\frac{dQ}{dP} \right) dQ \quad (6)$$

and we declare that $H(Q\|P) = \infty$ if Q does not have a density with respect to P . Again it follows from the strict convexity of the exponential function that equality is achieved if and only if the new random variable

$$Z = W + \sigma^{-1} \log \left(\frac{dQ}{dP} \right)$$

251 is Q -almost surely constant. This gives us the following variational characterization of the cumulant
252 generating function that is due to [40]:

Variational formula for the cumulant generating function. Let W be bounded from above, with $\mathbf{E}[\exp(-\sigma W)] < \infty$. Then

$$\gamma(\sigma) = \inf_{Q \ll P} \left\{ \int W dQ + H(Q\|P) \right\}, \quad (7)$$

where the infimum runs over all probability measures Q that have a density with respect to P . Moreover the minimizer Q^* exists and is given by

$$dQ^* = e^{\gamma(\sigma) - \sigma W} dP.$$

253 6. Optimal driving from control theory

254 When X_t denotes stochastic dynamics such as (1), the above variational formula admits a nice
255 interpretation in terms of an optimal control problem with a quadratic cost. To reveal it we first need
256 some technical assumptions.

(A1) We define $Q = [0, T) \times O$ where $T \in [0, \infty]$ and $O \subset \mathbb{R}^n$ is a bounded open set with smooth boundary ∂O . Further let $\tau < \infty$ be the stopping time

$$\tau = \inf \{ t > t_0 : (t, X_t) \notin Q \},$$

257 i.e. τ is the stopping time that either $t = T$ or X_t leaves the set O , whichever comes first.

(A2) The random variable W is of the form

$$W = \frac{1}{\epsilon} \int_0^\tau f(X_t) dt + \frac{1}{\epsilon} g(X_\tau),$$

258 for some continuous and nonnegative functions $f, g: \mathbb{R}^n \rightarrow \mathbb{R}$ which are bounded from above and
259 at most polynomially growing in x (compare Jarzyski's formula).

260 (A3) The potential $V: \mathbb{R}^n \rightarrow \mathbb{R}$ in (1) is smooth, bounded below, and satisfies the usual local Lipschitz
261 and growth conditions.

We consider the conditioned version of the moment generating function (which is just the exponential of the cumulant generating function):

$$\psi_\sigma(x, t) = \mathbf{E}[\exp(-\sigma W) | X_t = x]. \quad (8)$$

By the Feynman-Kac theorem, ψ_σ solves the linear boundary value problem

$$\begin{aligned} \left(\mathcal{A} - \frac{\sigma}{\epsilon} f\right) \psi_\sigma &= 0 \\ \psi_\sigma|_{E^+} &= \exp\left(-\frac{\sigma}{\epsilon} g\right) \end{aligned} \quad (9)$$

where E^+ is the terminal set of the augmented process (t, X_t) , precisely $E^+ = ([0, T) \times \partial O) \cup (\{T\} \times O)$, and

$$\mathcal{A} = \frac{\partial}{\partial t} + L \quad (10)$$

is the backward evolution operator associated with X_t and L the generator of the dynamics as introduced in (2). Assumptions (A1)–(A3) guarantee that (9) has a unique smooth solution ψ_σ for all $\sigma > 0$. Moreover the stopping time τ is almost surely finite which implies that

$$0 < c \leq \psi_\sigma \leq 1$$

262 for some constant $c \in (0, 1)$.

Log transformation of the cumulant generating function. In order to arrive at the optimal control version of the variational formula (7), we introduce the logarithmic transformation of ψ_σ as

$$v_\sigma(x, t) = -\frac{\epsilon}{\sigma} \log \psi_\sigma(x, t),$$

which is analogous to the CGF γ except for the leading factor ϵ and the dependence on the initial condition x . As we will show below, v_σ is related to an optimal control problem. To see this, remember that ψ_σ is bounded away from zero and note that

$$-\frac{\epsilon}{\sigma} \psi_\sigma^{-1} \mathcal{A} \psi_\sigma = \mathcal{A} v_\sigma - \sigma |\nabla v_\sigma|^2,$$

which implies that (9) is equivalent to

$$\begin{aligned} \mathcal{A} v_\sigma - \sigma |\nabla v_\sigma|^2 + f &= 0 \\ v_\sigma|_{E^+} &= g. \end{aligned}$$

Equivalently,

$$\begin{aligned} \min_{\alpha \in \mathbb{R}^n} \left\{ \mathcal{A} v_\sigma + \alpha \cdot \nabla v_\sigma + \frac{1}{4\sigma} |\alpha|^2 + f \right\} &= 0 \\ v_\sigma|_{E^+} &= g, \end{aligned} \quad (11)$$

where we have used that

$$-\sigma |y|^2 = \min_{\alpha \in \mathbb{R}^n} \left\{ \alpha \cdot y + \frac{1}{4\sigma} |\alpha|^2 \right\}.$$

263 (For the general framework of change-of-measure techniques and Girsanov transformations and their
264 relation to logarithmic transformations, we refer to [41, Sec. VI.3].)

Optimal control problem. Equation (11) is a Hamilton-Jacobi-Bellman (HJB) equation and is recognized as the dynamic programming equation of the following optimal control problem: minimize

$$J(u, x) = \mathbf{E} \left[\int_0^\tau \left\{ f(X_t) + \frac{1}{4\sigma} |u_t|^2 \right\} dt + g(X_\tau) \middle| X_t = x \right] \quad (12)$$

over a suitable space of admissible control functions $u: [0, \infty) \rightarrow \mathbb{R}^n$ and subject to the dynamics

$$dX_t = (u_t - \nabla V(X_t)) dt + \sqrt{2\epsilon} dW_t. \quad (13)$$

Form of optimal control. In more detail one can show (e.g., see [41, Sec. IV.2]) that assumptions (A1)–(A3) above imply that (11) has a classical solution (i.e. twice differentiable in x , differentiable in t and continuous at the boundaries), which satisfies $v_\sigma(x) = \min_u J(u, x)$, i.e.

$$v_\sigma(x, t) = \mathbf{E} \left[\int_t^\tau \left\{ f(X_s) + \frac{1}{4\sigma} |u_s^*|^2 \right\} ds + g(X_\tau) \middle| X_t = x \right], \quad (14)$$

where u^* is the unique minimizer of $J(u, \cdot)$ that is given by the Markovian feedback law

$$u_t^* = \alpha^*(X_t, t)$$

with

$$\alpha^* = \operatorname{argmin}_{\alpha \in \mathbb{R}^n} \left\{ \alpha \cdot \nabla v_\sigma + \frac{1}{4\sigma} |\alpha|^2 \right\}.$$

265 The function v_σ is called *value function* or *optimal-cost-to-go* for the optimal control problem (12)–
 266 (13). Specifically, $v_\sigma(x, t)$ measures the minimum cost needed to drive the system to the terminal state
 267 when started at x at time t . We briefly mention the two most relevant special cases of (12)–(13).

268 6.1. Case I: the exit problem

We want to consider the limit $T \rightarrow \infty$. To this end call $\tau_O = \inf\{t > 0: X_t \notin O\}$ the first exit time of the set $O \subset \mathbb{R}^n$. The stopping time $\tau = \min\{T, \tau_O\}$ then converges to τ_O , i.e.

$$\min\{T, \tau_O\} \rightarrow \tau_O.$$

As a consequence (using monotone convergence), v_σ converges to the value function of an optimal control problem with cost functional

$$J_\infty(u, x) = \mathbf{E} \left[\int_0^{\tau_O} \left\{ f(X_t) + \frac{1}{4\sigma} |u_t|^2 \right\} dt + g(X_{\tau_O}) \middle| X_t = x \right] \quad (15)$$

In this case $v_\sigma = \min_u J_\infty$ is *independent* of t and solves the boundary value HJB equation

$$\begin{aligned} \min_{\alpha \in \mathbb{R}^n} \{ L v_\sigma + \alpha \cdot \nabla v_\sigma + \frac{1}{4\sigma} |\alpha|^2 + f \} &= 0 \\ v_\sigma|_{\partial O} &= g. \end{aligned} \quad (16)$$

269 **6.2. Case II: finite time horizon optimal control**

If we keep $T < \infty$ fixed while letting O grow such that $\text{diam}(O) \rightarrow \infty$, where $\text{diam}(O) = \sup\{r > 0 : \mathcal{B}_r(x) \subset O, x \in O\}$ is understood as the maximum radius $r > 0$ that an open ball $\mathcal{B}_r(\cdot)$ contained in O can have, it follows that

$$\min\{T, \tau_O\} \rightarrow T$$

In this case v_σ converges to the value function with a finite time horizon and cost functional

$$J_T(u, x) = \mathbf{E} \left[\int_0^T \left\{ f(X_t) + \frac{1}{4\sigma} |u_t|^2 \right\} dt + g(X_T) \middle| X_t = x \right] \quad (17)$$

Now $v_\sigma = \min_u J_T$ is again a function on $\mathbb{R}^n \times [0, T]$ and solves the HJB equation

$$\begin{aligned} \min_{\alpha \in \mathbb{R}^n} \{ \mathcal{A}v_\sigma + \alpha \cdot \nabla v_\sigma + \frac{1}{4\sigma} |\alpha|^2 + f \} &= 0 \\ v_\sigma(x, T) &= g(x), \end{aligned} \quad (18)$$

270 with a terminal condition at time $t = T$.

271 **6.3. Optimal control potential and optimally controlled dynamics**

The optimal control u^* that minimizes the functional in (12) is again of gradient form and given by

$$u_t^* = -2\sigma \nabla v_\sigma(X_t, t)$$

as can be readily checked by minimizing the corresponding expression in (11) over α . Given v_σ , the *optimally controlled dynamics* reads

$$dX_t = -\nabla U(X_t, t) dt + \sqrt{2\epsilon} dW_t, \quad (19)$$

with the *optimal control potential*

$$U(x, t) = V(x) + 2\sigma v_\sigma(x, t). \quad (20)$$

272 In case when $T \rightarrow \infty$ (case I above), the biasing potential is independent of t .

273 **Remarks.** Some remarks are in order.

(a) Monte-Carlo estimators of the conditional CGF

$$\gamma(\sigma; x) = -\sigma^{-1} \log \mathbf{E}[\exp(-\sigma W) | X_0 = x],$$

274 that are based on the optimally controlled dynamics have zero variance. This is so because the
 275 optimal control minimizes the variational expression in (7), but at the minimum the random
 276 variable inside the expectation must be almost surely constant (as a consequence of Jensen's
 277 inequality and the strict convexity of the exponential function). Hence we have a *zero-variance*
 278 *estimator* of the conditional CGF.

279 (b) The reader may now wonder as to whether it is possible to extract single moments from the CGF
 280 (e.g., mean first passage times). In general this question is not straightforward to answer. One
 281 of the difficulties is that extracting moments from the CGF requires to take derivatives at $\sigma = 0$,
 282 but small values of σ imply strong penalization which renders the control inactive and thus makes
 283 the approach inefficient. Another difficulty is that reweighting the controlled trajectories back
 284 to the original (equilibrium) path measure can increase the variance of a rare event estimator, as
 285 compared to the corresponding estimator based on the uncontrolled dynamics. As yet, the efficient
 286 calculation of moments from the CGF by either extrapolation methods or reweighing is an open
 287 question and currently a field of active research (see, e.g., [42,43])

(c) Jarzynski's identity relates equilibrium free energies to averages that are taken over an ensemble of trajectories generated by controlled dynamics, and the reader may wonder whether the above zero-variance property can be used in connection with free energy computations à la Jarzynski. Indeed we can interpret the CGF as the free energy of the nonequilibrium work

$$W_\xi = \int_0^T f(X_t, \xi_t) dt$$

where f is the nonequilibrium force exerted on the system under driving it with some prescribed protocol $\xi: [0, T] \rightarrow \mathbb{R}$; in this case the dynamics X_t depends on ξ_t as well, and writing down the HJB equation according to (18) is straightforward. But even if we can solve (18) we do not get zero-variance estimators for the free energy

$$F(\xi_T) - F(\xi_0) = -\beta^{-1} \log \mathbf{E}[\exp(-\beta W_\xi)].$$

The reason for this is simple: Jarzynski's formula requires that the initial conditions are chosen from an equilibrium distribution, say, π_0 the equilibrium distribution corresponding to the initial value ξ_0 of the protocol, but optimal controls are defined point-wise for each state (t, X_t) and

$$\begin{aligned} & -\beta^{-1} \log \int_{\mathbb{R}^n} \mathbf{E}[\exp(-\beta W_\xi) | X_0 = x] d\pi_0(x) \\ & \neq -\beta^{-1} \int_{\mathbb{R}^n} \log \mathbf{E}[\exp(-\beta W_\xi) | X_0 = x] d\pi_0(x). \end{aligned}$$

In other words:

$$F(\xi_T) - F(\xi_0) \neq \int_{\mathbb{R}^n} V_\beta(x, 0) d\pi_0(x).$$

288 (d) A similar argument as the one underlying the derivation of the HJB equation from the linear
 289 boundary value problem yields that Jarzynski's formula can be interpreted as a two-player
 290 zero-sum differential game (cf. [44]).

291 7. Characterize Rare Events by Optimally Controlled MD

292 Now we illustrate how to use the results of the last section in practice. We will mainly consider the
 293 case discussed in Sec. 6.1 regarding the statistical characterization of hitting a certain set.

294 *7.1. First passage times*

Roughly speaking, the CGF encodes information about the moments of any random variable W that is a functional of the trajectories $(X_t)_{t \geq 0}$. For example, for $f = \epsilon$ and $T \rightarrow \infty$ we obtain the CGF of the mean first exit time from O , i.e.,

$$-\sigma^{-1} \log \mathbf{E}_x[\exp(-\sigma\tau_O)] = \min_u \mathbf{E}_x^u \left[\tau_O + \frac{1}{4\sigma} \int_0^{\tau_O} |u_t|^2 dt \right]$$

where we have introduced the shorthand $\mathbf{E}_x[\cdot] = \mathbf{E}[\cdot | X_0 = x]$ to denote the conditional expectation when starting at $X_0 = x$ and the superscript “ u ” to indicate that the expectation is understood with respect to the controlled dynamics

$$dX_t = (u_t - \nabla V(X_t)) dt + \sqrt{2\epsilon} dW_t,$$

295 where $\mathbf{E} = \mathbf{E}^0$ denotes expectation with respect to the unperturbed dynamics.

296 *7.2. Committed probabilities revisited*

It is not only possible to use the moment generating function to collect statistics about rare events in terms of the cumulant generating function, but also to express the committor function directly in terms of an optimal control problem (see Section 2.1 for the definition of the committor q_{AB} between to sets A and B). To this end, let $\sigma = 1$ and suppose we divide ∂O into two sets $B \subset \partial O$ and $A = \partial O \setminus B$ (i.e., τ_O is the stopping time that is defined by hitting either A or B). Setting

$$f = 0 \quad \text{and} \quad g(x) = -\epsilon \log \mathbf{1}_B(x)$$

reduces the moment generating function (8) to

$$\psi_1(x) = \mathbf{E}_x[\mathbf{1}_B(X_{\tau_O})]$$

or, in more familiar terms,

$$\psi_1(x) = \mathbf{P}[X_{\tau_O} \in B \wedge X_{\tau_O} \notin A | X_0 = x] = q_{AB}(x).$$

According to (15) the corresponding optimal control problem has the cost functional

$$J(u) = \mathbf{E} \left[\frac{1}{4} \int_0^{\tau_O} |u_s|^2 ds - \epsilon \log \mathbf{1}_B(X_{\tau_O}) \right],$$

which amounts to a control problem with zero terminal cost when ending up in B and an infinite terminal cost for hitting A . Therefore the HJB equation for $v = v_1$ has a singular boundary value at A ; it reads

$$\min_{\alpha \in \mathbb{R}^n} \left\{ Lv + \alpha \cdot \nabla v + \frac{1}{4} |\alpha|^2 \right\} = 0$$

$$v|_A = \infty, \quad v|_B = 0.$$

Setting $v(x) = -\epsilon \log q_{AB}(x)$ yields the equality

$$-\log q_{AB}(x) = \min_u \mathbf{E}_x^u \left[\frac{1}{4\epsilon} \int_0^{\tau_O} |u_s|^2 ds - \log \mathbf{1}_B(X_{\tau_O}) \middle| x_0 = x \right].$$

In this case, the optimally controlled dynamics (19) is of the form

$$dX_t = -\nabla U_{AB}(X_t)dt + \sqrt{2\epsilon}dW_t,$$

with optimal control potential

$$U_{AB}(x) = V(x) - 2\epsilon \log q_{AB}(x).$$

297 **Remarks.** Some remarks on the committor equation follow:

298 (a) The logarithmic singularity of the value function at “reactant state” A has the effect that the control
 299 will try to avoid running back into A , for there is an infinite penalty on hitting A . In other
 300 words, by controlling the system we condition it on hitting the “product state” B at time $t = \tau_O$.
 301 Conditioning a diffusion (or general Markov) process on an exit state has strong connection with
 302 Doob’s h-transform that can be considered a change-of-measure transformation of the underlying
 303 path measure that forces the diffusion to hit the exit state with probability one [45].

(b) The optimally controlled dynamics has a stationary distribution with a density proportional to

$$\exp(-\beta U_{AB}(x)) = q_{AB}^2(x) \exp(-\beta V(x)),$$

304 where we used $\beta = 1/\epsilon$.

7.3. *Algorithmic Realization* For the exit problem (“Case I” above), one can find an efficient algorithm for computing the conditional CGF $\gamma(\sigma; x)$ or, equivalently, the value function $v_\sigma(x)$ in [46]. The idea of the algorithm is to exploit that, according to (19)–(20), the optimal control is of gradient form. The latter implies that the value function can be represented as a minimization of the cost functional over time-homogeneous candidate functions C for the optimal bias potential, in other words,

$$v_\sigma(x) = \min_C \mathbf{E}_x \left[\int_0^{\tau_O} \left\{ f(X_t) + \frac{1}{4\sigma} |\nabla C_t|^2 \right\} dt + g(X_{\tau_O}) \right], \quad (21)$$

where the expectation \mathbf{E} is understood with respect to the path measure generated by

$$dX_t = -(\nabla C(X_t) + \nabla V(X_t)) dt + \sqrt{2\epsilon}dW_t.$$

Once the optimal C has been computed, both value function and CGF can be recovered by setting

$$v_\sigma(x) = -\frac{C(x)}{2\sigma} \quad \text{and} \quad \gamma(\sigma; x) = -\frac{C(x)}{2\epsilon\sigma}.$$

The algorithm that finds the optimal C works by iteratively minimizing the cost functional for potentials C from a finite-dimensional ansatz space, i.e.

$$C(x) = \sum_{j=1}^M a_j \varphi_j(x)$$

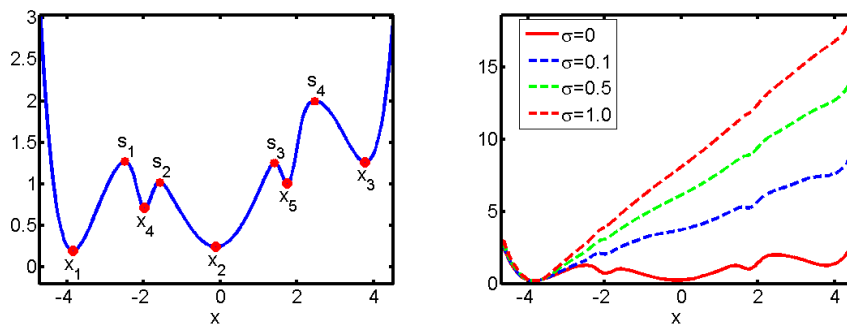
305 with appropriately chosen ansatz functions φ_j . The iterative minimization is then carried out on the M -
 306 dimensional coefficient space of the a_1, \dots, a_M . With this algorithm we are able to compute the optimal
 307 control potential for the exit problem in the two interesting cases: first passage times and committor
 308 probabilities (as outlined in Sections 7.1 and 7.2).

309 **Remark.** The minimization algorithm for the value function belongs to the class of expectation-
 310 maximization algorithms (although here we carry out a minimization rather than a maximization), in
 311 that each minimization step is followed by a function evaluation that involves computing an expectation.
 312 In connection with rare events sampling and molecular dynamics problems a close relative is the *adaptive*
 313 *biasing force* (ABF) method for computing free energy profiles, the latter being intimately linked with
 314 cumulant generating functions or value functions (cf. Section 5). In ABF methods (or its variants, such as
 315 *metadynamics* or *Wang-Landau dynamics*), the gradient of the free energy is estimated on the fly, running
 316 a molecular dynamics simulation, and then added as a biasing force to accelerate the sampling in the
 317 direction of the relevant coordinates [47,48]. The biasing force eventually converges to the derivative of
 318 the free energy, which is the optimal bias for passing over the relevant energy barriers that are responsible
 319 for the rare events [49].

320 7.4. Numerical Examples

321 In our first example we consider diffusive molecular dynamics as of (1) with $\epsilon = 0.1$ and V being
 322 the 5-well potential shown in Fig. 2. We first consider the CGF of the first passage time as discussed
 323 in Section 7.1. The resulting optimal control potential as of (20) is displayed in Fig. 2 for different σ .
 324 As the set O we take the whole state space except a small neighbourhood of its global minimum of V ,
 325 so that its complement O^c is identical to the vicinity of the global minimum and the exit time τ_O is the
 326 first passage time to O^c . Fig. 2 shows that the optimal control potential alters the original potential V
 327 significantly in the sense that for $\sigma > 0$ the set O^c is the bottom of the only well of the potential, so that
 328 all trajectories started somewhere else will quickly enter O^c .

Figure 2. Five-well potential (left) and associated optimal control potential for the first passage time to the target set O^c given by a small ball around the main minimum x_1 (right) for different values of σ (right). $\epsilon = 0.1$.

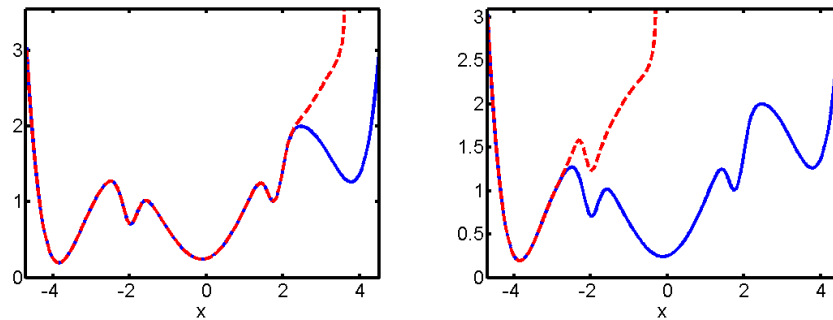


329 This case is instructive: For the unperturbed original dynamics the mean first passage time $\mathbf{E}_x(\tau_O)$
 330 takes values of around 10.000 for $x > -2$. For the optimally controlled dynamics the mean first passage
 331 times into O^c are less than 5 for $\sigma = 0.1, 0.5, 1.0$ so that the estimation of $\mathbf{E}_x(\tau_O)$ resulting from the
 332 optimal control approach requires trajectories that are a factor of at least 1.000 shorter than the ones we
 333 would have to use by direct numerical simulation of the unperturbed dynamics.

334 Figure 3 shows the optimal control potentials for computation of the committor q_{AB} as described in
 335 Section 7.2. We observe that the optimal control potential exhibits a singularity at the boundary of the

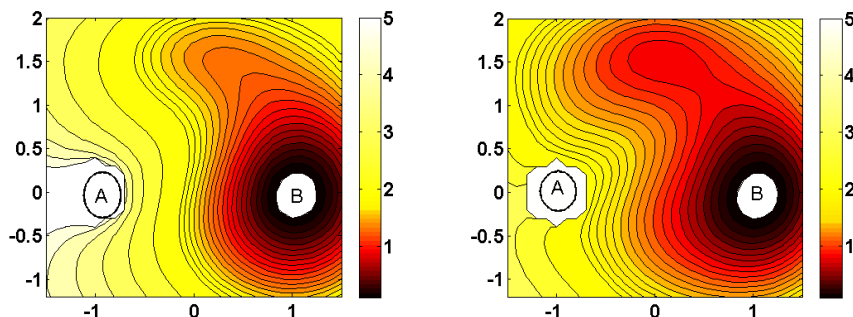
336 basin of attraction of the set A . That is, it prevents the optimally controlled dynamics from entering the
 337 basin of attraction of A and thus avoids the waste of computational effort by unproductive returns to A .

Figure 3. Optimally corrected potential for the case of J being the committor q_{AB} for B being the set around an 0.1-ball around the main minimum x_1 of the potential. Left panel: A =ball with radius 0.1 around the highest minimum x_3 . Right panel: A =ball with radius 0.1 around the second lowest minimum x_2 .



338 In our second example we consider two-dimensional diffusive molecular dynamics as of (1) with the
 339 energy landscape V being the 3-well potential shown in Fig. 1. In Fig. 4 the optimal control potential
 340 for computing the committors q_{AB} between the two main wells for two different temperatures $\epsilon = 0.15$
 341 and $\epsilon = 0.6$ are displayed. As in our former experiment we observe that the optimal control potential
 342 prevents the dynamics from returning to A ; in addition it flattens the third well significantly such that
 343 the optimally controlled dynamics in any case quickly goes into B . For $\epsilon = 0.15$ a TPS sampling of
 344 reactive trajectories between the two main wells, precisely from A to B with A and B as indicated in
 345 Fig. 4, results in an average length of 367 for reactive trajectories based on the original dynamics. For
 346 the optimally controlled dynamics we found an average length of 1.3.

Figure 4. Optimally corrected potential for the three well potential shown in Fig. 1 for the committor q_{AB} for the medium temperature $\epsilon = 0.6$ case (left) and the low temperature $\epsilon = 0.15$ case (right) and for the sets A (ellipse in main well, right hand side) and B (ellipse in main well, left hand side).



347 8. Conclusions

348 We have surveyed various techniques for the characterization and computation of rare events
349 occurring in molecular dynamics. Roughly, the approaches fall into two categories: (a) methods that
350 approach the problem by characterizing the ensemble of reactive trajectories between metastable states or
351 (b) path-based methods that target dominant transition channels or pathways by minimization of suitable
352 action functionals. Methods of the first type, e.g. Transition Path Theory, Transition Path Sampling,
353 Milestoning or variants thereof, are predominantly Monte-Carlo-type methods for generating one very
354 long or many short trajectories, from which the rare event statistics can then be estimated. Methods
355 that belong to the second category, e.g., MaxFlux, Nudged-Elastic Band or the String Method, are
356 basically optimization methods (sometimes combined with a Monte-Carlo scheme); here the objectives
357 are few (single or multiple) smooth pathways that describe, e.g. a transition event. It is clear that
358 this classification is not completely unambiguous, in that action-based methods for computing most
359 probable pathways can be also used to sample an ensemble of reactive trajectories. Another possible
360 classification (with its own drawbacks) is along the lines of the equilibrium-nonequilibrium dichotomy
361 that distinguishes between methods that characterize rare events based on the original dynamics
362 and methods that bias the underlying equilibrium distribution towards a (nonequilibrium) probability
363 distribution under which the rare events are no longer rare. Typical representatives of the second class
364 are methods based on Jarzynski's identity for computing free energy profiles. The problem often is that
365 rare event estimators based on an ensemble of nonequilibrium trajectories suffer from large variances,
366 unless the nonequilibrium perturbation is cleverly chosen.

367 We have described a strategy to find such a cleverly chosen perturbation, based on ideas from optimal
368 control. The idea rests on the fact that the cumulant generating function of a certain observable, e.g. the
369 first exit time from a metastable set, can be expressed as the solution to an optimal control problem which
370 yields a zero variance estimator for the cumulant generating function. The control acting on the system
371 has essentially two effects: (1) under the controlled dynamics, the rare events are no longer rare, as a
372 consequence of which the simulations become much shorter, (2) the variance of the statistical estimators
373 is small (or even zero if the optimal control is known exactly). We should stress that, depending on the
374 type of observable, the approach only appears to be a nonequilibrium method, for the optimal control is
375 an exact gradient of a biasing potential, hence the optimally perturbed system satisfies detailed balance
376 which is one criterion for thermodynamic equilibrium. Future research should address the question as
377 to whether the approach is competitive for realistic molecular systems, how to efficiently and robustly
378 extract information about specific moments rather than cumulant generating functions, and how to extend
379 it to more general observables or the calculation of free energy profiles.

380 References

- 381 1. Eyring, H. The Activated Complex in Chemical Reactions. *J. Chem. Phys.* **1935**, *3*, 107–115.
- 382 2. Wigner, E. Calculation of the Rate of Elementary Association Reactions. *J. Chem. Phys.* **1937**,
383 *5*, 720–725.
- 384 3. Bolhuis, P.G.; Chandler, D.; Dellago, C.; Geissler, P. Transition path sampling: throwing ropes
385 over mountain passes, in the dark. *Annu. Rev. Phys. Chem.* **2002**, *59*, 291.

- 386 4. E, W.; Ren, W.; Vanden-Eijnden, E. Probing multiscale energy landscapes using the string
387 method. *Phys. Rev. Lett.* **2002**. eprint arXiv:cond-mat/0205528.
- 388 5. Beccara, S.; Skrbic, T.; Covino, R.; Faccioli, P. Dominant folding pathways of a WW domain.
389 *PNAS* **2012**, *109*(7).
- 390 6. Faccioli, P.; Lonardi, A.; Orland, H. Dominant reaction pathways in protein folding: a direct
391 validation against molecular dynamics simulations. *J. Chem. Phys.* **2010**, *133*.
- 392 7. Pinski, F.; Stuart, A. Transition paths in molecules: gradient descent in path space. *J. Chem.*
393 *Phys.* **2010**, *132*, 184104.
- 394 8. Allen, R.; Warren, P.; ten Wolde, P.R. Sampling rare switching events in biochemical networks.
395 *Physical Review Letters* **2005**, *94*, 018104: 1–4.
- 396 9. Moroni, D.; van Erp, T.; Bolhuis, P. Investigating rare events by transition interface sampling.
397 *Physica A* **2004**, *340*, 395.
- 398 10. Faradjian, A.K.; Elber, R. Computing time scales from reaction coordinates by milestoning. *J.*
399 *Chem. Phys.* **2004**, *120*, 10880–10889.
- 400 11. Olender, R.; Elber, R. Calculation of classical trajectories with a very large time step: Formalism
401 and numerical examples. *J. Chem. Phys.* **1996**, *105*, 9299–9315.
- 402 12. Jarzynski, C. Nonequilibrium Equality for Free Energy Differences. *Phys. Rev. Lett.* **1997**,
403 *78*, 2690–2693.
- 404 13. Crooks, G. Entropy production fluctuation theorem and the nonequilibrium work relation for free
405 energy differences. *Physical Review E* **1999**, *60*, 2721.
- 406 14. Sarich, M.; Bansich, R.; Hartmann, C.; Schuette, C. Markov State Models for Rare Events in
407 Molecular Dynamics. *Entropy* **2013**, (*submitted*).
- 408 15. E, W.; Vanden-Eijnden, E. Metastability, conformation dynamics, and transition pathways in
409 complex systems. Multiscale modelling and simulation. Springer, Berlin, 2004, Vol. 39, *Lect.*
410 *Notes Comput. Sci. Eng.*, pp. 35–68.
- 411 16. E, W.; Vanden-Eijnden, E. Towards a theory of transition paths. *Journal of statistical physics*
412 **2006**, *123*, 503–523.
- 413 17. Metzner, P.; Schütte, C.; Vanden-Eijnden, E. Illustration of Transition Path Theory on a
414 Collection of Simple Examples. *J. Chem. Phys.* **2006**, *125*. 084110.
- 415 18. E, W.; Vanden-Eijnden, E. Transition-Path Theory and Path-Finding Algorithms for the Study of
416 Rare Events. *Annual Review of Physical Chemistry* **2010**, *61*, 391–420.
- 417 19. Metzner, P.; Schütte, C.; Vanden-Eijnden, E. Transition Path Theory for Markov Jump Processes.
418 *Multiscale Modeling and Simulation* **2009**, *7*, 1192–1219.
- 419 20. Metzner, P. Transition Path Theory for Markov Processes: Application to molecular dynamics.
420 PhD thesis, Free University Berlin, 2007.
- 421 21. Noé, F.; Schütte, C.; Vanden-Eijnden, E.; Reich, L.; Weikl, T. Constructing the full ensemble of
422 folding pathways from short off-equilibrium trajectories. *PNAS* **2009**, *106*(45), 19011–19016.
- 423 22. Bolhuis, P.G.; Dellago, C.; Chandler, D.; Geissler, P. Transition path sampling: Throwing ropes
424 over mountain passes, in the dark. *Ann. Rev. of Phys. Chem.* **2001**. in press.
- 425 23. Chandler, D. *Finding transition pathways: throwing ropes over rough mountain passes, in the*
426 *dark*; World Scientific: Singapore, 1998.

- 427 24. Berkowitz, M.; Morgan, J.D.; McCammon, J.A.; Northrup, S.H. Diffusion-controlled reactions:
428 A variational formula for the optimum reaction coordinate. *J. Chem. Phys.* **1983**, *79*, 5563–5565.
- 429 25. Huo, S.; Straub, J.E. The MaxFlux algorithm for calculating variationally optimized reaction
430 paths for conformational transitions in many body systems at finite temperature. *J. Chem. Phys.*,
431 **1997**, *107*, 5000–5006.
- 432 26. Zhao, R.; Shen, J.; Skeel, R.D. Maximum Flux Transition Paths of Conformational Change. *J.*
433 *Chem. Theory Comput.* **2010**, *6*, 2411–2423.
- 434 27. Cameron, M. Estimation of reactive fluxes in gradient stochastic systems using an analogy with
435 electric circuits. *J. Comput. Phys.* **2013**, *247*, 137–152.
- 436 28. Ren, W.; Vanden-Eijnden, E. String method for the study of rare events. *Phys. Rev. B* **2002**.
437 eprint arXiv:cond-mat/0205528.
- 438 29. Jonsson, H.; Mills, G.; Jacobsen, K. Nudged Elastic Band Method for Finding Minimum Energy
439 Paths of Transitions. *Classical and Quantum Dynamics in Condensed Phase Simulations*. World
440 Scientific, 1998. B. J. Berne, G. Ciccotti and D. F. Coker, editors.
- 441 30. Freidlin, M.; Wentzell, A.D. *Random perturbations of dynamical systems*; Springer, New York,
442 1998.
- 443 31. Ren, W.; Vanden-Eijnden, E. Finite temperature string method for the study of rare events. *J.*
444 *Phys. Chem. B* **2005**, *109*.
- 445 32. Ren, W.; Vanden-Eijnden, E.; Maragakis, P.; E, W. Transition pathways in complex systems:
446 Application of the finite-temperature string method to the alanine dipeptide. *J. Phys. Chem.*
447 **2005**, *123*.
- 448 33. Vanden-Eijnden, E.; Venturoli, M. Revisiting the finite temperature string method for the
449 calculation of reaction tubes and free energies. *J. Phys. Chem.* **2009**, *130*.
- 450 34. Allen, R.; Frenkel, D.; ten Wolde, P.R. Simulating rare events in equilibrium or nonequilibrium
451 stochastic systems. *J. Chem. Phys.* **2006**, *124*, 024102.
- 452 35. Allen, R.; Frenkel, D.; ten Wolde, P.R. Forward flux sampling-type schemes for simulating rare
453 events: efficiency analysis. *J. Chem. Phys.* **2006**, *124*, 194111.
- 454 36. Vanden-Eijnden, E.; Venturoli, M.; Ciccotti, G.; Elber, R. On the assumptions underlying
455 milestoning. *J. Chem. Phys.* **2008**, *129*, 174102.
- 456 37. Latorre, J.; Hartmann, C.; Schuette, C. Free energy computation by controlled Langevin
457 processes. *Procedia Computer Science* **2010**, *1*, 1591–1600.
- 458 38. Lelièvre, T.; Stoltz, G.; Rousset, M. *Free Energy Computations: A Mathematical Perspective*;
459 Imperial College Press, 2010.
- 460 39. Isralewitz, B.; Gao, M.; Schulten, K. Steered molecular dynamics and mechanical functions of
461 proteins. *Curr. Opin. Struct. Biol.* **2001**, *11*, 224–230.
- 462 40. Dai Pra, P.; Meneghini, L.; Runggaldier, W. Connections between stochastic control and dynamic
463 games. *Math. Control Signals Systems* **1996**, *9*, 303–326.
- 464 41. Fleming, W.; Soner, H. *Controlled Markov Processes and Viscosity Solutions*; Springer, 2006.
- 465 42. Awad, H.; Glynn, P.; Rubinstein, R. Zero-Variance Importance Sampling Estimators for Markov
466 Process Expectations. *Math. Oper. Res.* **2013**, *38*, 358–388.

- 467 43. Badowski, T. *Importance sampling using discrete Girsanov estimators*; PhD Thesis, FU Berlin:
468 Freie Universität Berlin, in preparation.
- 469 44. Fleming, W. Risk sensitive stochastic control and differential games. *Commun. Inf. Syst.* **2006**,
470 *6*, 161–178.
- 471 45. Day, M. Conditional exits for small noise diffusions with characteristic boundary. *Ann. Probab.*
472 **1992**, *20*, 1385–1419.
- 473 46. Hartmann, C.; Schütte, C. Efficient rare event simulation by optimal nonequilibrium forcing. *J.*
474 *Stat. Mech. Theor. Exp.* **2012**, p. 11004.
- 475 47. Darve, E.; Rodriguez-Gomez, D.; Pohorille, A. Adaptive biasing force method for scalar and
476 vector free energy calculations. *J. Chem. Phys.* **2008**, *128*, 144120.
- 477 48. Lelièvre, T.; Rousset, M.; Stoltz, G. Computation of free energy profiles with parallel adaptive
478 dynamics. *J. Chem. Phys.* **2007**, *126*, 134111.
- 479 49. Lelièvre, T.; Rousset, M.; Stoltz, G. Long-time convergence of an adaptive biasing force methods.
480 *Nonlinearity* **2008**, *21*, 1155–1181.

481 © July 23, 2013 by the authors; submitted to *Entropy* for possible open access
482 publication under the terms and conditions of the Creative Commons Attribution license
483 <http://creativecommons.org/licenses/by/3.0/>.